

# A Numerical Simulation of Horizontal Axis Hydrokinetic Turbine with and without Augmented Diffuser

Cristian Cardona-Mancilla\*, Jorge Sierra-Del Rio\*\*<sup>‡</sup>, Diego Hincapié-Zuluaga\*\*, Chica E.\*\*\*

\* Instituto Tecnológico Metropolitano, Facultad de Ingeniería, Former Student, 050034, Postal code

\*\* Instituto Tecnológico Metropolitano, Facultad de Ingeniería, Professor, 050034, Postal code

\*\*\* Departamento de Ingeniería Mecánica, Facultad de Ingeniería, Universidad de Antioquia UdeA, Calle 70, No. 52-21, Medellín, Colombia. 050034, Postal code

(cristiancardona@itm.edu.co, jorgesierra@itm.edu.co, diegohincapie@itm.edu.co, edwin.chica@udea.edu.co)

<sup>‡</sup>Corresponding Author; Jorge Sierra Del Rio, Calle 73 No. 76A-354, Vía al Volador, Tel: + 57301 357 4232, jorgesierra@itm.edu.co

*Received: 27.06.2018 Accepted: 24.09.2018*

**Abstract-** The hydrodynamic analysis of a horizontal axis hydrokinetic turbine is carried out, using a 3rd-generation diffuser. The turbine constituted of three blades and a radius of 0.75 m, using the hydrodynamic profile NREL S822 for the design of both the blades and the housing of the 3rd generation diffuser. Two horizontal axis hydrokinetic turbine with and without diffuser were meshed and subsequently hydrodynamically simulated using the ANSYS CFX 18.2® program in a transient state. As a result, the power coefficient ( $C_p$ ) of the turbine was obtained with and without a diffuser, in addition to the velocity profile of each model. The maximum power coefficient ( $C_{P,max}$ ) reached by the turbine with and without diffuser is 0.487 at a TSR of 9.948, and 0.285 at a TSR of 10.472, respectively, equivalent to an increase of 71% of  $C_p$  with respect to the turbine without diffuser, and 82.1% with relation to the Betz limit. Speeds are reached between 1.5 to 2.1 m/s and 1.5 to 1.8 m/s, upstream of the turbine with and without diffuser, respectively, and from 2.3 to 2.6 m/s and 1.8 to 2.1 m/s downstream of it, in the same order.

**Keywords** CFD, distributed-generation, kinetic energy, renewable energy.

## 1. Introduction

The hydrokinetic turbines emerge with the goal of using the kinetic energy in marine currents, rivers, artificial channels and others, without interrupting the water's natural flow, directly transforming it in mechanical power. These mechanisms require simple infrastructures for their work, due to their independence of high heads require very little civil work compared to dams, generating low implementation costs and times, and a minimal environmental impact [1], [2]. However, the main disadvantage of these devices with respect to the conventional hydroelectric centrals, is the low energy density that can be obtained; 35% efficiency, considerably low if

compared to the 80-90% efficiency of that of hydro power plants. Therefore, there is a constant search for improvement in order to increase their physical and economical feasibility, [3], [4].

The energy predictability of hydrokinetic turbines is similar to that of hydro power plants, and both hinder navigation and fishery in the areas where they have been installed. Nonetheless, hydrokinetic turbines have wider range of applicability, for example, they can be installed in remote-off-grid areas, high seismic risk areas, and highly populated areas.

There are several kinds of hydrokinetic turbines, differing in sizes and energy capture principles. The major

classification of hydrokinetic turbines has to do with the rotating axis positions with respect to the water flow: a) horizontal axis hydrokinetic turbines (HAHTs), where the rotational axis must be oriented in parallel with regard to the water current in order to produce power; and b) vertical axis hydrokinetic turbines (VAHTs), where the rotational axis is perpendicular to the water current direction [4]–[6].

It is noteworthy that numerous sources claim that HAHTs have a major efficiency per same swept area. Nevertheless, the main advantage of VAHTs is that the blades can have a constant shape along their length and, unlike HAHTs, twisting the blade is not required, as every section of the blade is subjected to the same water speed; allowing an easier design, fabrication and replication of the blade, which results in cost reduction. Nonetheless, VAHTs are not as efficient as HAHTs and they exhibit problems such as self-starting resonance at a particular rotational speed, poor starting torque and torque fluctuations, or torque ripple of the turbine due to the blades passing in and out of torque-generating regions. These cyclic loads are of concern when designed for turbine reliability and longevity. These VAHTs' problems are the main reason why HAHTs are preferred for hydrokinetic energy conversion systems, despite the higher manufacturing costs. To avoid the disadvantages of VAHTs, different hydrofoil profiles, helical blade configuration, and increased number of blades with variable pitch might be used to reduce the shaking of the blades while maintaining a strong starting torque and high peak power coefficient [2], [5], [7].

In 1987 the first hydrokinetic turbine appeared, developed by the investigation group of the Mechanic Department from the University of Brasilia (UnB) [8]. From this turbine, diverse prototypes were produced to generate an operative turbine, being finally started up on in July 1995 to supply the electric energy of a medical place in Correntina, BA. This turbine, constituted by an axial rotor of 2 blades, a diameter of 800 mm and a blade solidity of 30%, has the capability of generating 1.5 kW at flow speeds of 2 m/s, and was denominated as "1st generation". Later, improvements were applied on this kind of turbines, being one of the main modifications the installation of a conical diffuser, supported by their similarity, of the advances obtained with this kind of mechanism on wind turbines. This system was denominated as "2nd generation". This device produces a decrease in the downstream pressure of the turbine, generating an increase in the upstream flow speed, allowing to enhance its power coefficient. The lower outlet pressure induces a greater mass flow through the turbine and enable a turbine to surpass Betz limit. Finally, the technological advances have allowed designing a hydrokinetic turbine of "3rd generation", or hydrokinetic turbine with augmented diffuser, whose goal is to improve its hydrodynamic performance. This system is constituted by an integrated mechanic system with a serial disposition, where the first of them surrounds the rotor, with the shape of an outlined casing that at the same time acts as diffuser, and the second, a diffuser split in the posterior zone of the turbine and the casing as can be seen in Fig. 1. The hydrodynamic performance increase in this improvement is mainly due to an existing opening between the casing and the diffuser at a radial level, that allows the flow to go from the

exterior to the interior of the diffuser, increasing the fluid's energy downstream of the turbine by momentum conservation law inside the control volume of the study, where the external fluid prints a drag towards the outlet of the fluid that goes through the turbine, with this could be controlled the limit layer in the inside surface of the diffuser in this zone, avoiding recirculation currents that are associated to energy losses in the fluid. The integration of both components allows using a shorter diffuser with a higher opening angle, becoming a cheaper option with respect to the diffusers of older generations. Another important aspect that is searched in 3rd generation turbines is to promote a compact system [9]; therefore, the generator becomes a set with the rotor when it is integrated with the core of the latter, which decreases the energy losses associated to elements of power transmission. With the implementation of this device, a hydraulic efficiency close to 90% can be reached [10], respect to the Betz limit.

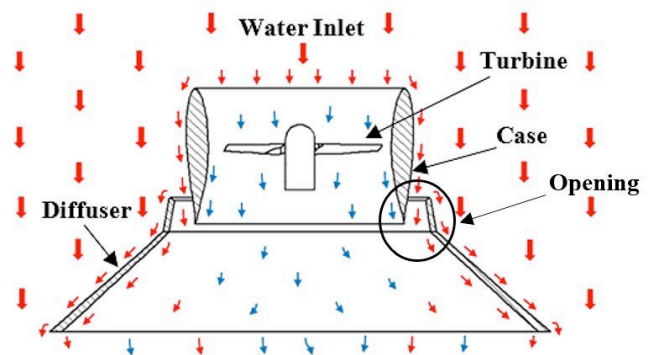


Fig. 1. Hydrodynamic design of a hydrokinetic turbine with horizontal axis and 3rd generation diffuser. Own source.

A similar study with 3rd generation diffusers is performed by Piancastelly, Clarke, and Cassani, [11] who computationally designed and analyzed a mechanism of electric pico-generation, looking for an increase in the power of the hydrokinetic turbines; two models are proposed, being the first one design with a rectangular throat section for turbines with vertical axis, and the second one with circular section for turbines with horizontal axis. Both mechanisms have four improvements: (1) a convergent-divergent diffuser with shape of Venturi nozzle design under the specifications of the standard DIN EN ISO 5167-3:2003, (2) a second diffuser that surrounds the first device, (3) an S-flange at the outlet of the second diffuser, and (4) a divergent internal diffuser downstream of the turbine. This mechanism manages to increase 2.25 and 2.33 times the flow speed for the first and second model, respectively, representing in this same order an increase of 11.4 and 12.7 times the generated power.

There are several practical advantages in placing the turbine in a diffuser. The diffuser eliminates tip losses on axial flow turbine blades, improving efficiency. In areas with risk of animals and/or floating debris being drawn into the turbine, a grid could be placed on the upstream opening of the diffuser, thus increasing the lifespan of the turbine and avoiding damaging or clogging it [12]–[14]. The diffuser shades the turbine from direct sunlight, and weed growth will

thereby be reduced. Along with floating debris, this was one of the major problems turbines can experience [3], [7], [15].

The main objective of this study consists in performing the hydrodynamic analysis through computational simulation of a horizontal axis hydrokinetic turbine, where a 3rd generation diffuser is implemented in order to increase the efficiency of this kind of turbines and foment their use as renewable energy source.

## 2. Theory

The hydrokinetic turbines have the same functioning principles if the wind turbines, sharing a similar design philosophy. The design of hydrokinetic turbines with horizontal axis starts from the sizing of the rotor, so its power ( $P$ ) is calculated by Eq.1 as a function of the fluid's density ( $\rho$ ), the area swept by the blade of the rotor ( $A = \pi R^2$ ), where  $R$  is the radius of the turbine, the fluid's speed ( $V$ ), the power coefficient ( $C_p$ ) and the efficiency of the mechanism's drivetrain ( $\eta$ ) related to gears, generator, and others, being considered in this work for the latter a value of 70%, according to the reference [16].

$$P = \frac{1}{2} \rho \pi R^2 V^3 C_p \eta \quad (1)$$

The performance of the hydrokinetic turbine is characterized by its power coefficient ( $C_p$ ) (Eq.2), that represents the relation between the extracted power of the current of water and the available power in the current that goes through the same area projected by the turbine [17]. This implies that the turbine cannot fully extract the contained energy in the water flow, so the limit established by Betz for this  $C_p$  is 0.593 [4], [15], [18], [19].

$$C_p = \frac{P}{0.5 \rho \pi R^2 V^3} \quad (2)$$

This coefficient depends at the same time of the TSR (Tip Speed Ratio) represented by  $\lambda$ . For this reason, the existing ratio between the speed of the blade in the tip and the water current, has a big influence in the turbine's efficiency, being a fundamental factor that must be maximized to obtain the best possible power coefficient and optimize the extraction of the contained energy in these currents [16]. This relation is defined through Eq.3, where  $R$  represents the radius of the turbine,  $\omega$  the angular velocity of the rotor and  $V$  the fluid velocity [20], [21].

$$\lambda = \frac{R\omega}{V} \quad (3)$$

An expansion on the Betz law to include fluid dynamic components near the rotor plane has been theorized by Jamieson et al. [22] and Werle & Presz, [23] showing that exceeding the Betz limit is possible. Some authors [3], [24], have attributed the exceeding of the Betz limit to the

upstream effect a diffuser experience by increasing the mass flow through the rotor and hence the velocity.

## 3. Methodology

The elaboration and attachment of the tridimensional models of the hydrokinetic turbine with horizontal axis and 3rd generation diffuser, as well as their respective fluid volumes, was performed using the software NX10.0® of Siemens. The computational models for the study of the turbine were developed with and without diffuser, constituted in both cases by one rotative and one stationary volume (Fig. 2); according to the studies performed by [16], [25].

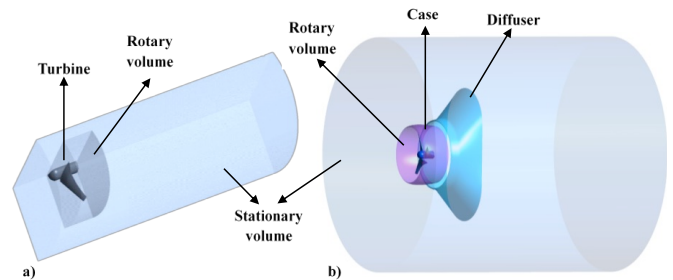


**Fig. 2.** Fluid volume of the horizontal axis hydrokinetic turbine: (a) without diffuser and (b) with 3rd generation diffuser.

The design of the turbine consists of three blades, using for them the hydrodynamic profile NREL S822, an angle of attack of  $5^\circ$  and a radius of 0.75 m. For the horizontal shaft hydrokinetic turbine without diffuser, a geometric simplification was used to a 3rd of the same to reduce computational costs, taking advantage of the geometric and dynamic symmetry presented by it. To ensure that the walls of the fluid volume do not affect the flow profile that interacts with the turbine, a stationary volume with the dimensions shown in Fig. 3a was configured for the turbine without diffuser, where  $R$  denotes the radius of the turbine. For this, a distance greater than  $1 R$  was respected, as established by Kolekar & Banerjee, [26], from the end of the blades to the outer wall of the stationary volume. For the second model, a 3rd generation diffuser was implemented on the hydrokinetic turbine used in the first model, where, as in the previous model, measures greater than  $1 R$  of the outer fluid walls were guaranteed with respect to the most exterior walls of the diffuser, as can be seen in Fig. 3b, while the rotary volume adopted the same shape of the inner part of the 3rd generation diffuser. These dimensions have values higher than those used for the model of the turbine without diffuser, because the components cover a larger area and, for the same flow conditions, the profile of the boundary layer that appears at the outlet of the diffuser, it is farthest from the axis of the turbine, which is why this stationary volume must be greater, guaranteeing that wall effects do not affect the flow, as recommended in the literature.

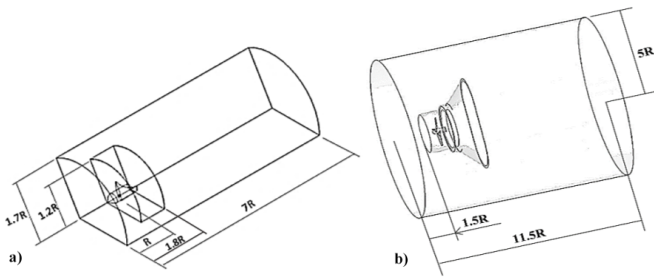


**Fig. 3.** Dimensions of the fluid volumes of the horizontal axis hydrokinetic turbine: (a) without diffuser and (b) with 3rd generation diffuser, depending on the radius [R] of the turbine.

The configured diffuser for this study consists of two elements, a profiled housing that surrounds the rotor, which was designed using the hydrodynamic profile NREL S822, also used in the blades of the turbine for its self-cleaning characteristics [16] and a diffuser located at the exit of the housing. A geometric simplification, such as that used for the turbine without diffuser, is not performed on this model, because the turbine-diffuser set does not present a plane of similarity. The model of the hydrokinetic turbine with a 3rd generation diffuser, as well as its dimensions, is presented in Fig. 4.

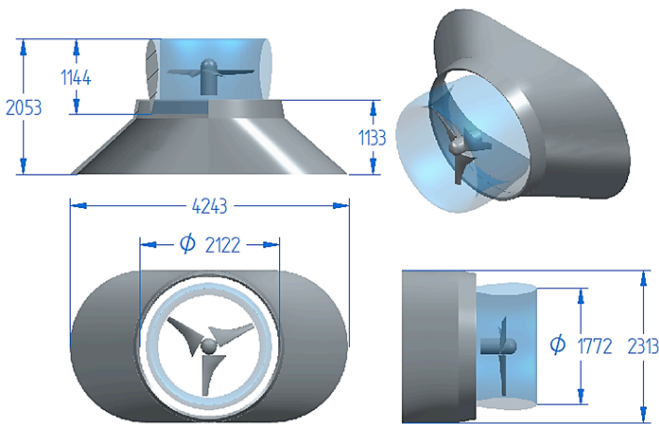


**Fig. 4.** 3rd generation hydrokinetic turbine and its dimensions in millimeters (mm).

The volumes of fluid were exported to the commercial program ANSYS® V18.2, where their preprocessing was performed, starting from the definition of the regions of interest of each domain and the subsequent subdivision of these by the generation of the mesh. An unstructured mesh consisting mainly of tetrahedral elements was used for both models, and the size of the mesh elements was adjusted to the trailing edge of the blade to 1 mm. This is to satisfy the Y+ requirement of the configured turbulence model, given that in this area there is a release of boundary layer and instabilities in the fluid. For the turbine without diffuser, a proximity and curvature algorithm was used, with a minimum mesh size of 5 mm, a maximum face size of 10 mm and a maximum size of tetrahedron of 20 mm. While, for the turbine with diffuser, a curvature algorithm was applied, with a minimum mesh size of 40 mm, a face maximum of 50 mm and a maximum tetrahedron size of 60 mm. Values that were established after performing the

respective mesh independence study for both models. The number of mesh nodes used was  $3.6218E + 06$  and  $3.6684E + 06$ , for the turbine with and without diffuser, respectively.

The CFD analysis (Computational Fluid Dynamics) was performed in the CFX module of the ANSYS® V18.2 software. The computational model was configured for a transient state characterized by a total time of 6 s and 4 s of operation for the turbine models with and without diffuser, respectively. A time step of  $1.0E-02$  s was used for the analysis of both models, guaranteeing maximum RMS values lower than  $1.0E-04$  as convergence criterion in conservation of mass and momentum. Torque monitors in the axis of the turbine were configured to quantify their temporal variation, allowing to determine the stability in the behavior of this, which verifies the change from transient to stationary state in the operation of the turbine, guaranteeing a fully developed flow [27]. Water was set as the work fluid at room temperature. The interface between the walls of the rotating volume and the stationary one was established as "frozen rotor" according to the reference [28], besides the implementation of the turbulence model k-ε, according to the studies performed by Chica et al., [16] and Gaden & Bibeau, [3]. A double precision study was used in CFX-Solver, to reduce numerical errors. Fig. 5 shows a block diagram with the configuration of the parameters used for analysis both at the input and the output in the simulation environment (in general), water input speed of 1.5 m/s and a variation of the angular velocity from 0 to 160 RPM, with steps of 10 RPM

were used.

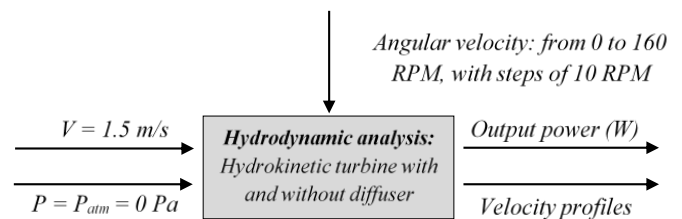


**Fig. 5.** Design of experiments by blocks of the hydrodynamic analysis.

#### 4. Results

Fig. 6 shows the Power Coefficient ( $C_p$ ) of the hydrokinetic turbine with and without diffuser as a function of the TSR ( $\lambda$ ) for a range of angular velocity between 0 and 160 RPM with steps of 5 RPM. The results show a parabolic behavior of the  $C_p$  with respect to the variation of the TSR, consistent with the numerical and experimental results available in the literature for this kind of turbines [26], [29]. In the case of the turbine without diffuser, the maximum  $C_p$  reached is 0.285 at a TSR of 10.472, while the  $C_p$  for the turbine with diffuser is 0.487 at a TSR of 9.948. This is equivalent to an increase of 71% of the power coefficient of the hydrokinetic turbine, by using the proposed 3rd generation diffuser, which represents an efficiency of 82.1% with respect to the Betz limit.



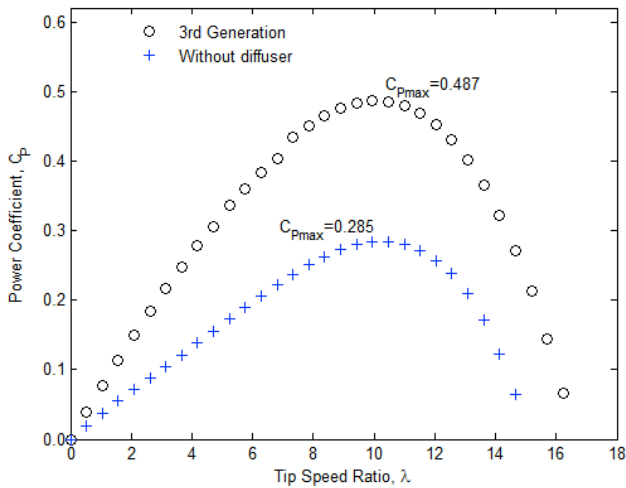


**Fig. 6.** Variation of the power coefficient ( $C_p$ ) as a function of the tip speed ratio ( $\lambda$ ) for a hydrokinetic turbine without diffuser (+) and with a 3rd generation diffuser (o).

The increase of the efficiency of the 3rd generation turbines corresponds to the additional external inlet flow that injects kinetic energy downstream of the turbine. Consequently, an increase of the velocity flow across the turbine can be obtained. This phenomenon does not occur in first nor in second generation turbines because of the geometric configuration as can be seen in the schematic figure 7. In addition, in second generation turbines, the fluid experiences an adverse pressure gradient due to the recirculation zone behind the diffuser, close to the turbine, which can be associated with energy losses [3].

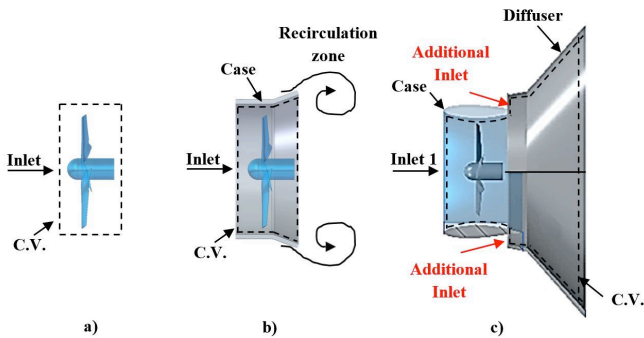


**Fig. 7.** Schematic configuration: a) 1st; b) 2nd and c) 3rd generation turbines.

Fig. 8 shows the contours and velocity vectors (m/s) in the middle cross section of the blade of the turbine with and without diffuser (Fig. 8a and Fig. 8b, respectively), at a distance measured from the tip of the blade of 0.306 m. Both velocity profiles comprise a color scale with values between 0 and 2.6 m/s. Higher velocity is shown upstream of the turbine, in the middle area of the blade profile and lower velocity downstream of it, in addition to an acceleration of the fluid in the outer lateral zones of the inlet and outlet edges of the hydrodynamic profile, once it goes through the blade. Also, for both models, a detachment of the boundary layer in the profile of the turbine blade is presented, due to

the high velocity of water at the inlet and the rotational velocity of the blade, which is greater in the upper part, causing an increase of layer detachment in this area. The velocity vectors show, for both cases, a normal flow behavior both upstream of the turbine, and in areas where the blade does not affect the passage of water, however, there is a phenomenon of recirculation downstream of this, in the middle area of the blade. Both the release of the boundary layer, and the recirculation of water, generate energy losses in the mechanism.

There is an increase in the velocity at the inlet of the turbine, generated by the implementation of the diffuser (Fig. 8a) with speeds between 1.5 and 2.1 m/s, while the turbine without diffuser (Fig. 8b) has lower velocity values in the same zones with speeds between 1.5 and 1.8 m/s. It is also found that, in both cases, the velocity of the fluid decreases both in the upper and lower areas where the profile of the turbine blade is located, which is coherent given the restriction that is generated by the passage of water. However, there is an increase in velocity downstream of the blade, in areas where there is no direct incidence of this, which increases as it moves away from the hydrodynamic profile. The flow velocities in these zones are more homogeneous and again higher for the turbine with diffuser, with values between 2.3 and 2.6 m/s, with respect to those reached by the turbine without diffuser with a range between 1.8 and 2.1 m/s. The velocities downstream of the profile show a greater stagnation of water for the turbine without diffuser (Fig. 8b), presenting in a more homogeneous and concentrated manner, velocities between 0 and 0.5 m/s. While, for the turbine with diffuser, the speeds oscillate between 0 and 0.8 m/s, appreciating a smaller area in which the fluid reaches its minimum value of speed, with respect to that presented by the turbine without diffuser in these same zones.

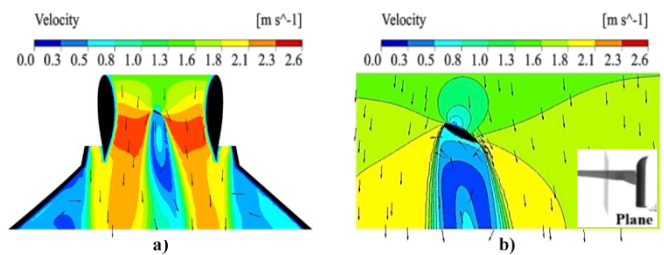


**Fig. 8.** Contour and velocity vectors (m/s) in the middle cross section of the turbine blade: a) with diffuser and b) without diffuser.

To determine the speed difference between both models, the average speed was calculated on a plane located at the diffuser exit and respecting for the turbine without diffuser the same distance with respect to the lower base of the cube of 0.114 m, obtaining values of 1.64 and 1.55 m/s, for the turbine with and without diffuser, respectively. Corresponding to an increase in the average speed of the fluid downstream of the turbine of 5.8%.

Fig. 9 shows the contours and velocity vectors in the mean cross section of the turbine model with and without a diffuser (Fig. 9a and Fig. 9b, respectively). Both velocity profiles comprise a color scale with values between 0 and 2.6

m/s. Higher speeds are shown upstream of the turbine, in the middle area of the blade profile and lower speeds downstream of it, in addition to an acceleration of the fluid in the outer lateral zones of the inlet and outlet edges of the hydrodynamic profile, once it goes through the blade.

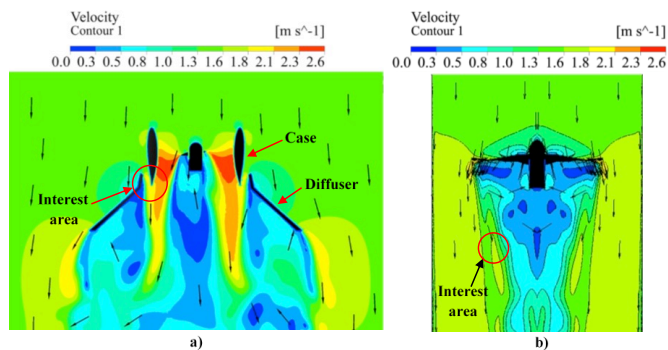


**Fig. 9.** Contour and velocity vectors (m/s) in the middle cross section of the turbine blade: a) with diffuser and b) without diffuser.

Fig. 9a shows that, the opening between the casing and the diffuser (area of interest) allows the external fluid to enter the turbine and the casing, increasing the speed inside the mechanism, by injecting kinetic energy by dragging of the external fluid to the internal one that passes through the turbine, going from 1.5 to 2.1 m/s when the diffuser is installed, which prevents the recirculation of fluid at the outlet edge of the casing profile, contributing also to control and improve the performance of the same to avoid the release of boundary layer in this area, as was raised in the study of Els & Junior, [10]. This increase in the velocity of the fluid generates a greater thrust of the flow downstream of the turbine with respect to the turbine without diffuser, which it is possible to evacuate in greater proportion the water held there or recirculating. While the turbine without diffuser (Fig. 9b), presents downstream of the turbine, in the same area of interest, speeds between 1.3 and 1.8 m/s.

There are not enough studies in the literature related to the implementation of 3rd generation diffusers in hydrokinetic turbines, which are necessary to perform a qualitative validation of the results obtained. The study developed by Piancastelli et al., [11] shows a great similarity with respect to the objective of the present work, which proposes a similar mechanism, that differs basically in the geometric configuration of a 3rd diffuser downstream of the turbine of the model in comparison. The improvements of diffuser augmented proposed by Piancastelli et al., [11] shape a mechanism of great similarity to the 3rd-generation diffuser (Fig. 4) analyzed in the present study, making possible a qualitative comparison between both models. In their study, the authors reached an increase of speed up to a maximum of 2.25 times. On the other hand, the proposed turbine of 3rd generation allowed to reach average speeds of 2.5 m/s downstream of the turbine, representing an increase of the speed of 67% in relation to the initial velocity of the fluid of 1.5 m/s. This indicates that the model proposed by Piancastelli et al., [11] presents an increase of 31.4% in fluid velocity compared to that generated by the 3rd-generation diffuser.

The difference in the speed increases presented by the mechanism proposed by reference [11] and the 3rd generation diffuser proposed in the present work can be linked mainly to two factors, the first one based on the geometric differences that the diffusers of both models present, and the second is about not taking into account the turbine in the hydrodynamics analysis of the device proposed by [11] which does not quantify the energy loss by the fluid-rotor interaction.

From both studies it is shown that, the implementation of two or more diffusers allows to increase the power coefficient ( $C_p$ ) of hydrokinetic turbines with values higher than 0.4, which was possible thanks to the increase of the speed downstream of the turbine by reducing the zones of stagnation and fluid recirculation. It is important to remark that, an increase in the flow speed across the turbine does not mean an increase in the turbine efficiency. Piancastelli et al., [11] found a ( $C_p$ ) of 0.41 for increases of 2.25 times of the velocity, whereas the ( $C_p$ ) obtained by the proposed design corresponds to 0.487 for an increase of 1.7 times in the velocity across the turbine.

## 5. Conclusions

A CFD study was performed in order to determine the efficiency in a hydrokinetic 3rd generation turbine, composed mainly by an augmented diffuser, which allows inlet the external flow directly downstream of the turbine. Efficiency comparisons between a turbine with and without augmented diffuser determined the possibility of implementing this device in hydrokinetic turbines to enhance their efficiency. The hydrokinetic turbine shows a better performance when implementing the proposed configuration, achieving an increase of 71% of the power coefficient ( $C_p$ ) in relation with the turbine without diffuser, which represents an efficiency of 82.1% with respect to the maximum energy capacity that can be obtained from this type of mechanisms, established by the Betz limit. In hydrokinetic turbines applications, the inclusion of an augmented diffuser translates into a smaller turbine, favoring spatial limitations at the design stage. The diffuser modeled in this study has a non-conventional geometry, however, further benefits are expected using flaps and turbulators at the case-diffuser ensemble.

## References

- [1] G. L. T. Filho, Z. De Souza, C. a B. De Rossi, R. M. Barros, and F. D. G. B. Da Silva, "Poraque" hydrokinetic turbine," *IOP Conf. Ser. Earth Environ. Sci.*, vol. 12, p. 12094, 2010.
- [2] M. I. Yuce and A. Muratoglu, "Hydrokinetic energy conversion systems: A technology status review," *Renew. Sustain. Energy Rev.*, pp. 72–82, 2015.
- [3] D. L. F. Gaden and E. L. Bibeau, "A numerical investigation into the effect of diffusers on the performance of hydro kinetic turbines using a

- validated momentum source turbine model,” *Renew. Energy*, vol. 35, no. 6, pp. 1152–1158, Jun. 2010.
- [4] M. J. Khan, G. Bhuyan, M. T. Iqbal, and J. E. Quaicoe, “Hydrokinetic energy conversion systems and assessment of horizontal and vertical axis turbines for river and tidal applications: A technology status review,” *Appl. Energy*, vol. 86, no. 10, pp. 1823–1835, 2009.
- [5] Y. M. A. Fatemeh Behrouzi, Mehdi Nakisa, Adi Maimun, “Global renewable energy and its potential in Malaysia: A review of Hydrokinetic turbine technology,” *Renew. Sustain. Energy Rev.*, vol. 2, p. pp 1270-1281, 2016.
- [6] M. J. Khan, M. T. Iqbal, and J. E. Quaicoe, “A technology review and simulation based performance analysis of river current turbine systems,” *2006 Can. Conf. Electr. Comput. Eng.*, no. May, pp. 2288–2293, 2006.
- [7] D. Kumar and S. Sarkar, “A review on the technology, performance, design optimization, reliability, techno-economics and environmental impacts of hydrokinetic energy conversion systems,” *Renew. Sustain. Energy Rev.*, vol. 58, pp. 796–813, 2016.
- [8] J. H. Harwood, “Protótipo de um cata-água que gera 1 kW de eletricidade,” *ACTA Amaz.*, vol. 15, pp. 403–412, 1985.
- [9] A. Agha, H. N. Chaudhry, and F. Wang, “Diffuser Augmented Wind Turbine (DAWT) Technologies: A Review,” *International*, vol. 8, no. 3, 2018.
- [10] R. H. Van Els and A. C. P. B. Junior, “The Brazilian Experience with Hydrokinetic Turbines,” *Energy Procedia*, vol. 75, pp. 259–264, 2015.
- [11] L. Piancastelli, R. V. Clarke, and S. Cassani, “Diffuser augmented run the river and tidal pico-hydropower generation system,” vol. 12, no. 8, pp. 2678–2688, 2017.
- [12] P. Romero-Gomez and M. C. Richmond, “Simulating blade-strike on fish passing through marine hydrokinetic turbines,” *Renew. Energy*, vol. 71, pp. 401–413, 2014.
- [13] M. Anyi and B. Kirke, “Evaluation of small axial flow hydrokinetic turbines for remote communities,” *Energy Sustain. Dev.*, vol. 14, no. 2, pp. 110–116, Jun. 2010.
- [14] M. Anyi and B. Kirke, “Tests on a non-clogging hydrokinetic turbine,” *Energy Sustain. Dev.*, vol. 25, pp. 50–55, Apr. 2015.
- [15] H. J. Vermaak, K. Kusakana, and S. P. Koko, “Status of micro-hydrokinetic river technology in rural applications: A review of literature,” *Renew. Sustain. Energy Rev.*, vol. 29, pp. 625–633, 2014.
- [16] E. Chica, F. Perez, A. Rubio-Clemente, and S. Agudelo, “Design of a hydrokinetic turbine,” *WIT Trans. Ecol. Environ.*, vol. 195, pp. 137–148, 2015.
- [17] L. A. Gish, A. Carandang, and G. Hawbaker, “Numerical Optimization of Pre-Swirl Stators for Horizontal Axis Hydrokinetic Turbines,” *Ocean. 2016 MTS/IEEE Monterey*, 2016.
- [18] M. S. Güney and K. Kaygusuz, “Hydrokinetic energy conversion systems: A technology status review,” *Renew. Sustain. Energy Rev.*, vol. 14, no. 9, pp. 2996–3004, Dec. 2010.
- [19] L. A. Gish and G. Hawbaker, “Experimental and Numerical Study on Performance of Shrouded Hydrokinetic Turbines,” *Ocean. 2016 MTS/IEEE Monterey*, 2015.
- [20] S. Hazim, A. EL Ouatuati, and M. T. Janan, “Modeling Approach for Hydrokinetic Turbine,” *2016 Int. Renew. Sustain. Energy Conf.*, no. 3, 2016.
- [21] M. Shahsavarifard, E. L. Bibeau, and A. H. Birjandi, “Performance gain of a horizontal axis hydrokinetic turbine using shroud,” *2013 Ocean. - San Diego*, pp. 0–4, 2013.
- [22] P. Jamieson, “Generalized Limits for Energy Extraction in a Linear Constant Velocity Flow field,” *Wind energy*, vol. 11, pp. 445–457, 2008.
- [23] W. M. Werle, M.J. & Presz, “Ducted Wind/Water Turbines and Propellers Revisited,” *J. Propuls. Power*, vol. 24, pp. 1146–1150, 2008.
- [24] A. Chica, E. Pérez, F., Rubio-Clemente, “Influence of the diffuser angle and a damper opening angle on the performance of a hydrokinetic turbine,” *Environ. Prog. Sustain. Energy*, vol. vol 37 (2), pp. 824–831, 2018.
- [25] W. C. Schleicher, J. D. Riglin, Z. a Kraybill, and G. Gardner, “Design and Simulation of a Micro Hydrokinetic Turbine,” *Proc. 1st Mar. Energy Technol. Symp. METS13*, 2013.
- [26] N. Kolekar and A. Banerjee, “Performance characterization and placement of a marine hydrokinetic turbine in a tidal channel under boundary proximity and blockage effects,” *Appl. Energy*, vol. 148, pp. 121–133, 2015.
- [27] Y. Castañeda Ceballos, M. Cardona Valencia, D. Hincapie Zuluaga, and J. Sierra del Rio, “Influence of the Number of Blades in the Power Generated by a Michell Banki Turbine,” *Int. J. Renew. Energy Res.*, vol. 7, no. 4, 2017.
- [28] S.-J. Kim, P. M. Singh, B.-S. Hyun, Y.-H. Lee, and Y.-D. Choi, “A study on the floating bridge type horizontal axis tidal current turbine for energy independent islands in Korea,” *Renew. Energy*, vol. 112, pp. 35–43, Nov. 2017.
- [29] W. C. Schleicher, J. D. Riglin, and A. Oztekin, “Numerical characterization of a preliminary portable micro-hydrokinetic turbine rotor design,” *Renew. Energy*, vol. 76, pp. 234–241, Apr. 2015.